Current Microbiology (2023) 80:126
https://doi.org/10.1007/s00284-023-03226-y

# Synergistic Effects of Baicalin and Levofloxacin Against Hypervirulent *Klebsiella pneumoniae* Biofilm In Vitro

**Jiahui Han[1] · Jin Luo[1] · Zhongye Du[1] · Yiqiang Chen[1] · Tangjuan Liu[1]**

Received: 14 November 2022 / Accepted: 12 February 2023 / Published online: 6 March 2023


## Abstract

Hypervirulent *Klebsiella pneumoniae* (hvKp) strains that form biofilms have recently emerged worldwide; however, the mechanisms underlying biofilm formation and disruption remain elusive. In this study, we established a hvKp biofilm model, investigated its in vitro formation pattern, and determined the mechanism of biofilm destruction by baicalin (BA) and levofloxacin (LEV). Our results revealed that hvKp exhibited a strong biofilm-forming ability, forming early and mature biofilms after 3 and 5 d, respectively. Early biofilm and bacterial burden were significantly reduced by BA + LEV and EM + LEV treatments, which destroyed the 3D structure of early biofilms. Conversely, these treatments were less effective against mature biofilm. The expression of both *AcrA* and *wbbM* was significantly downregulated in the BA + LEV group. These findings indicated that BA + LEV might inhibit the formation of hvKp biofilm by altering the expression of genes regulating efflux pumps and lipopolysaccharide biosynthesis.

## Introduction

*Klebsiella pneumoniae* is a gram-negative commensal bacterium and an important opportunistic pathogen causing severe, life-threatening infections of the respiratory, digestive, and urinary tracts [1]. In the era of antibiotics, *K. pneumoniae* became a major cause of healthcare-associated infections and a risk factor of severe community-acquired infections [2]. In China, *K. pneumoniae* infections accounted for 11.9% of cases of ventilator-associated pneumonia (VAP) and intensive care unit (ICU)-acquired pneumonia [3]. In Singapore, the mortality rates of *K. pneumoniae* bacteremia were reported to range from 20 to 26% [4]. Such high prevalence and mortality rates of *K. pneumoniae* infections undoubtedly cause a great burden on national health systems. In addition, *K. pneumoniae* continues to evolve and adapt as it acquires new genetic material. The two currently circulating *K. pneumoniae* pathotypes include the classical (cKp) and hypervirulent (hvKp) types [5]. In 1986, seven cases of invasive hvKp infection in individuals presenting with hepatic abscess in the absence of biliary tract disease and septic endophthalmitis were reported in Taiwan, China. Of note, hvKp is also known as hypermucoviscous *K. pneumoniae* (hmKp) because of its hypermucoviscous phenotype [6, 7]. This pathogen is more virulent than cKp and continues to evolve. Interestingly, hvKp is often detected in healthy populations, in which it causes severe, life-threatening, community-acquired infections characterized by pathological changes, such as septic liver abscess, meningitis, necrotizing fasciitis, and endophthalmitis. Over the last three decades, the incidence of hvKp infections has steadily increased, and they are now more common in Asia than in Western countries. Infections caused by hvKp have been reported in several regions of the world, including North America, South America, Europe, and Australia [8].

With the advancement of medical science and technology, medical devices and artificial organs are increasingly used for the treatment of various diseases [9]. Implants, such as catheters, dentures, artificial heart valves, and prostheses have been associated with biofilm-related infections [10]. The formation of bacterial biofilms is the primary means by which bacteria defend themselves against external stressors [11]. However, the broadly used therapeutic concentrations of antibiotics cannot usually eradicate the bacterial cells residing deep within the biofilm structure.

✉ Yiqiang Chen
chenyiq0708@163.com

✉ Tangjuan Liu
414413498@qq.com

[1] Department of Pulmonary and Critical Care Medicine, The First Affiliated Hospital of Guangxi Medical University, Nanning, Guangxi Zhuang Autonomous Region, People's Republic of China

In general, the antibiotic treatment of biofilms is protracted and requires high drug doses. Moreover, the overuse of antibiotics has increased antimicrobial resistance (AMR) globally [12]. Consequently, the world is on the verge of a postantibiotic era, with the spread of AMR potentially dramatically regressing medical care [13]. Thus, we need novel antimicrobial agents that can modulate/inhibit biofilm formation and overcome drug resistance in infectious diseases [14].

Several studies have recently reported on the ability of traditional Chinese medicine, such as *Scutellaria baicalensis*, to inhibit biofilm formation [15]. The plant's extract, especially its principle active ingredient, baicalin (BA), has attracted the research interest of pharmacologists. Baicalin is the main phytochemical marker in the quality control of *S. baicalensis*. This compound has antibacterial, antiallergic, antitumor, hepatoprotective, choleretic, immunomodulatory, antifungal, and antibacterial properties [16]. Baicalin is also known to work synergistically with various antibiotics, accelerating biofilm disruption, enhancing antibiotic penetration, and facilitating bacterial clearance [17]. Quinolone antibiotics, such as norfloxacin, ciprofloxacin, flurofloxacin, and levofloxacin (LEV), which target various gram-negative bacilli, are commonly used in the clinic. Levofloxacin is a third generation fluoroquinolone exhibiting both broad-spectrum and enhanced antibacterial activity [18]. Macrolides, such as erythromycin (EM), are broad-spectrum antibiotics with 14-, 15-, or 16-member macrocyclic lactone rings. Several studies have revealed that macrolides are potentially valuable in the treatment of biofilm-associated infections as they disrupt the bacterial biofilm and facilitate the bactericidal action of other antibiotics [19]. In particular, erythromycin has played an important role as an antibacterial agent since its initial discovery and clinical application [20]. Other representative macrolides include azithromycin and clarithromycin.

In the present study, we screened hvKp strains using the string test. We next evaluated the biofilm formation ability of hvKp strains using the Congo red agar method and semiquantitatively assessed biofilm generation by crystal violet staining. We also constructed a hvKp biofilm model and examined biofilm formation in vitro. To the best of our knowledge, no prior study has reported the effects of baicalin alone or in combination with other antibiotics, such as fluoroquinolones, cephalosporins, or aminoglycosides, on hvKp biofilm formation. This study aimed to establish a hvKp biofilm model, evaluate hvKp biofilm formation patterns in vitro, and investigate the effects of BA combined with LEV on hvKp biofilm formation and biofilm-related gene expression.

## Materials and Methods

### Reagents

Baicalin (BA, no. 190712; purity > 98%) was purchased from Refmedic (Nanjing, China). Levofloxacin (LEV, no. 130455–201607; purity > 98.5%) and erythromycin (EM, no. 130307–201417 purity > 98%) were provided by the China Institute of Pharmaceutical and Biological Products Inspection (Shanghai, China).

### Bacterial Strains

Between October 2019 and October 2020, 289 K. *pneumoniae* strains were isolated from clinical samples at the First Affiliated Hospital of Guangxi Medical University (Nanning, Guangxi, China). Duplicate strains from the same organs/tissues of the same patient were eliminated. Written informed consent for the provision and release of all clinical samples used in the study was obtained from all participants. Bacterial strains were identified using a VITEK-2 compact automatic bacterial identification drug sensitivity analyzer (bioMérieux SA, Marcy-l'Étoile, France). Isolated strains were inoculated in glycerol and frozen at − 80 °C. The *K. pneumoniae* ATCC43816 strain was provided by the Centre for Environmental Life Sciences Engineering Laboratory, Nanyang Technological University (Singapore, Singapore).

### hvKp Screening

We screened all hvKp strains using the "string test" [21]. Briefly, each lyophilized *K. pneumoniae* isolate was thawed, and a small amount of bacterial solution was obtained using a sterile inoculation loop. The bacterial solution was applied to Mueller–Hinton (MH) agar plates (Solarbio, Beijing, China) using the three-zone line method [21]. MH agar plates were then incubated at 37 °C for 24 h. After 24 h, the MH agar plates were removed and the colonies were touched with a sterile inoculation loop and drawn outwards. A positive result was indicated by the generation of a viscous string > 5 mm in length following the stretching of bacterial colonies on MH agar.

### Biofilm Formation Ability

#### Congo Red Agar Method of Qualitative Biofilm Formation

Selected hvKp isolates were inoculated on Congo red agar plates using the three-zone line method [22]. Accordingly, Congo red agar plates inoculated with bacteria were incubated at 37 °C for 24 h and the growth of colonies was

observed. Biofilm-positive strains on Congo red plates were indicated by small, dry, black colonies delineated by transparent circles (Fig. 1a), whereas large, red, mucoid, smooth, and rounded colonies indicated biofilm-negative strains.

### Semiquantitative Analysis of Biofilm Formation by Crystal Violet Staining

Evaluation of biofilm formation was performed in 96-well microtiter plates as previously described [22]. Briefly, 200 µl bacterial suspension (optical density $[OD]_{600} = 0.1$; ~ $10^8$ colony forming units [CFU]/ml) was added to each well. MH broth without bacterial suspension was used as the negative control. After incubation at 37 °C for 24 h, the plate was washed thrice with sterile distilled water, dried at 20–25 °C, and stained with 200 µl crystal violet (0.1% w/v) for 15 min. The excess stain was rinsed thrice with sterile distilled water, the plate was dried, and the bound stain was solubilized in 200 µl of 95% (v/v) ethanol. The solubilized stain in each well was transferred to a new microtiter plate, and its absorbance was measured at 570 nm ($OD_{570}$) using a microtiter plate reader (Multiskan; Thermo Fisher Scientific, Waltham, MA, USA). Tested strains were classified according to their ability to form biofilms, as previously described [22]. Averages were calculated from at least three independent trials.

OD ≤ OD cut-off (ODc) = not a biofilm former.
ODc < OD ≤ 2ODc = weak biofilm former.
2ODc < OD ≤ 4ODc = moderate biofilm former.
4ODc < OD = strong biofilm former.

The ODc value was defined as three standard deviations > the mean OD of the negative control.

### hvKp Biofilm Model Establishment

Based on the results of the crystal violet staining assay, the strain with the strongest biofilm formation ability, that is, hvKp1, was selected for the construction of the in vitro hvKp biofilm model, as previously described [17]. The hvKp1 strain was restored to an active state, and a bacterial suspension ($OD_{600} = 0.1$) was prepared. Each well of a 24-well plate (Corning Inc., Corning, NY, USA) was filled with 1 ml bacterial suspension and fitted with a PVC sheet serving as the biofilm growth carrier. The 24-well plate was then incubated at 37 °C, the MH broth was replaced every 24 h, and the biofilm was continuously cultured for 1–7 d before its growth was terminated and evaluated. The carrier was removed, semiquantitatively stained with crystal violet,

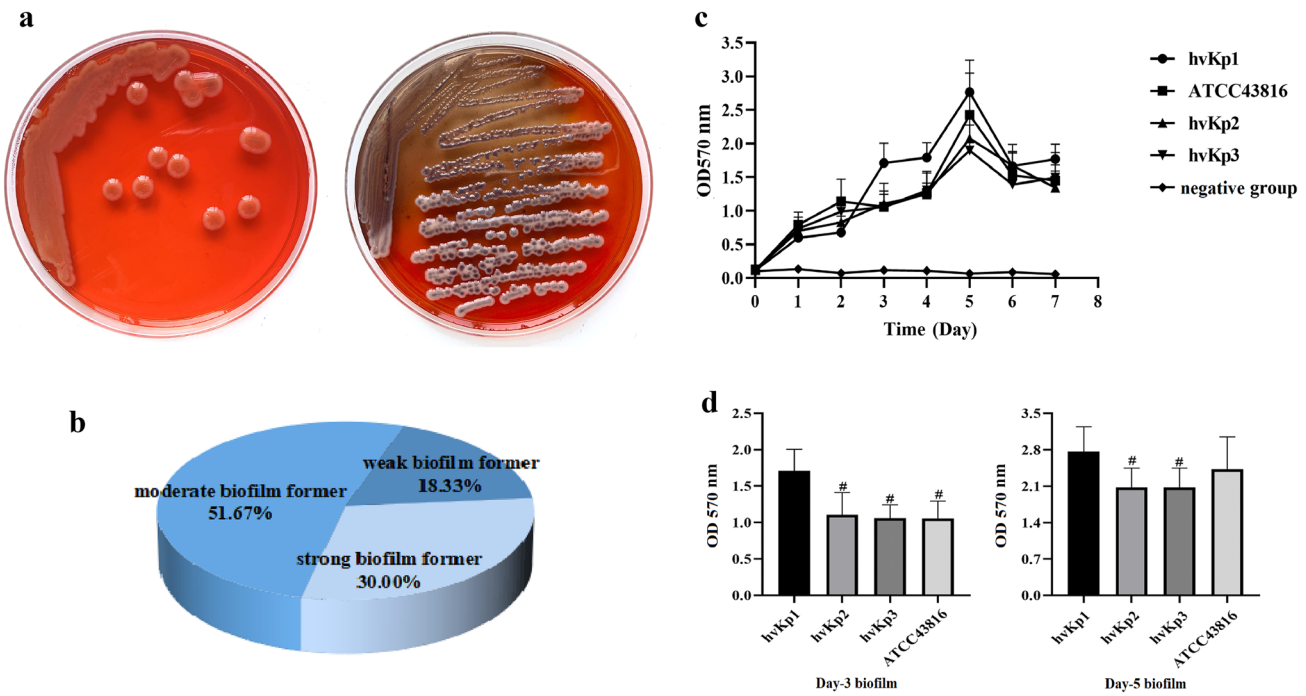


**Fig. 1** **a** Congo red agar method for biofilm formation (Small, dry, black colonies delineated by transparent circles indicated biofilm-positive strains and large, red, mucoid, smooth, rounded colonies indicated biofilm-negative strains.) **b** Analysis of the biofilm formation ability of biofilm-positive strains). **c** Growth curve of biofilm on carrier surfaces. hvKp: hypervirulent Klebsiella **d** Biofilm mass of hypervirulent Klebsiella pneumoniae (hvKp). # indicates $P < 0.05$ compared with hvKp1

and examined under a scanning electron microscope (SEM) (VEGA3 LMU; TESCAN, Brno, Czech Republic).

## Plotting of Biofilm Growth Curve

The carrier was removed, gently rinsed with sterilized phosphate-buffered saline (PBS), fixed with 2.5% (v/v) glutaraldehyde for 2 h, and dried. Subsequently, it was stained with 0.1% (w/v) crystal violet at 20–25 °C for 15 min, washed with sterilized PBS to remove any unbound crystal violet solution. The carrier was then decolorized with 95% (v/v) ethanol, and its absorbance was measured at 570 nm using a microtiter plate reader. Three parallel holes were made each day.

## Scanning Electron Microscopy Analysis

The carrier was removed, gently washed with sterilized PBS, fixed in 2.5% (v/v) glutaraldehyde solution, soaked in sterilized PBS, fixed in osmium tetroxide ($OsO_4$), and dehydrated in an ethanol gradient series (70, 80, 90, and 100% [v/v]). Subsequently, the carrier was dried under a vacuum (HCP-2 Critical Point Dryer, DAP-6D; ULVAC KIKO, Inc., Tokyo, Japan), sputter-coated with gold, and observed under a SEM (VEGA3 LMU; TESCAN) [17].

## Determination of Minimum Inhibitory Concentration

The minimum inhibitory concentrations (MICs) of BA, EM, and LEV were determined using the broth microdilution dilution method according to the guidelines of the Clinical and Laboratory Standards Institute (2019) [23]. ATCC43168 was used as the quality control strain. Briefly, serial twofold dilutions of BA, EM, and LEV were prepared in MH broth, and 100 µl of each dilution solution was added to each well of 96-well plates. Subsequently, 100 µl diluted bacterial suspension ($\sim \times 10^5$ CFU/ml) was added to each well containing the drug dilution. The control contained only inoculated MH broth. The 24-well plates were incubated at 37 °C for 24 h. The lowest concentration of the drug dilution resulting in no visible growth in the well was considered to be the MIC endpoint of the specific drug. In addition, the visual turbidity of each well was noted, both before and after incubation to confirm the obtained MIC value. The experiment was performed in triplicate.

## In Vitro Antibiofilm Effect Assay

Bacterial cultures at $OD_{600} = 0.1$ were prepared and transferred to each well of a 24-well plate (Corning Inc.). A PVC sheet was placed in each well and used as the biofilm growth carrier. The plate was incubated at 37 °C and 5% $CO_2$ atmosphere. The MH broth was replaced every other day until incubation was discontinued on days 3 and 5. Planktonic bacteria on the carrier surface were removed with sterilized PBS. MH broth and EM were used as the negative and positive controls, respectively. The following drug treatment groups were prepared: MH broth (MH); dimethyl sulfoxide (DMSO); BA at a final concentration of 1/4 MIC (BA); EM at a final concentration of 1/4 MIC (EM); LEV at a final concentration of MIC (LEV); LEV at a final concentration of twofold MIC (2LEV); BA plus LEV at a final concentration of MIC (BA + LEV); and EM plus LEV at a final concentration of MIC (EM + LEV). All treatments were applied for 24 h.

### Colony Count Assay

Bacteria in the biofilm were enumerated by the plate counting method [24]. After 24 h treatment, the carriers were removed, washed with sterilized PBS to remove planktonic bacteria, placed in tubes containing 1 ml of sterile physiological saline, and vortexed to release and disperse the bacteria. The original bacterial suspensions were serially diluted to various concentrations in sterile physiological saline. Ten microliters of each dilution were spread with a sterile coating bar onto MH agar plates and incubated at 37 °C for 24 h. Bacterial colony counts were expressed in $\log_{10}$ CFU/ml. The experiment was performed in triplicate.

### Semiquantitative Analysis of Biofilm Formation

Crystal violet staining [25] was used to quantify the generated biofilm mass. After 24 h treatment, the carrier was removed, washed with sterilized PBS to remove planktonic bacteria, dried at 20–25 °C, stained with 0.1% (w/v) crystal violet for 15 min, washed thrice with sterilized PBS, dried again at 20–25 °C, and placed in 95% (v/v) ethanol. The biomass was quantified by measuring its $OD_{570}$ using a microplate reader (Multiskan; Thermo Fisher Scientific). The experiment was performed in triplicate and in parallel.

**Table 1** Primers used for real-time quantitative PCR

| Primer | | Base sequence |
|---|---|---|
| *23srRNA* | *23srRNA*-F | ATCGTACCCCAAACCGACAC |
| | *23srRNA*-R | TTCTCCCGAAGTTACGGCAC |
| *wbbM* | *wbbM*-F | ATGCGGGTGAGAACAAACCA |
| | *wbbM*-R | AGCCGCTAACGACATCTGAC |
| *AcrA* | *AcrA*-F | CTCTGGCGGTCGTTCTGATGC |
| | *AcrA*-R | CATGTGCTGGGCTCCCTGTTG |
| *mrkA* | *mrkA*-F | ACGTCTCTAACTGCCAGGC |
| | *mrkA*-R | TAGCCCTGTTGTTTGCTGGT |

**Table 2** Distribution of hypervirulent *Klebsiella pneumoniae* strains among clinical departments

| Department | Value ($N=80$) | Department | Value ($N=80$) |
|---|---|---|---|
| Intensive care unit (ICU) | 18 (22.50) | Cardiothoracic surgery | 3 (3.75) |
| Respiratory medicine | 18 (22.5) | Hepatobiliary surgery | 8 (10.00) |
| Gastroenterology | 3 (3.75) | Neurosurgery | 6 (7.50) |
| Neurology | 3 (3.75) | Gastroenterology surgery | 2 (2.50) |
| Hematology | 2 (2.50) | Urology | 4 (5.00) |
| Medical oncology | 3 (3.75) | Burns and plastic surgery | 2 (2.50) |
| Endocrinology | 2 (2.50) | Traditional Chinese medicine | 1 (1.25) |
| Nephrology | 1 (1.25) | Rehabilitation medicine | 1 (1.25) |
| Cardiology | 1 (1.25) | Dermatology | 2 (2.50) |

Values are presented as No. (%) of isolates

## Relative Expression of the *wbbM*, *mrkA*, and *AcrA* Genes

### RNA Extraction and cDNA Synthesis

After 24 h of drug treatment, the carrier was removed, washed with sterilized PBS to remove planktonic bacteria, placed in a tube containing 1 ml sterile physiological saline, ultrasonicated for 10 min, and vortexed for 5 min for the release and dispersion of bacteria. Drug-free medium served as the control. Total bacterial RNA was extracted using the RNAiso Plus kit (Takara Bio Inc., Shiga, Japan) according to the manufacturer's instructions. Single-stranded cDNA was synthesized using the PrimeScript™ RT Master Mix (Takara Bio Inc.) according to the manufacturer's instructions.

### RT-qPCR

RT-qPCR was performed in a LightCycler480 System with TB Green® Premix Ex Taq™ II (Takara Bio Inc.) according to the manufacturer's instructions. The expression of the *wbbM*, *mrkA*, and *AcrA* genes was assessed by RT-qPCR using the 23S rRNA as an internal control. The primer sequences used in this experiment were reported in the literature and synthesized by Sangon Biotech [16], and are shown in Table 1. Cycling parameters were as follows: pre-denaturation stage at 95 °C for 30 s; polymerase chain reaction stage at 95 °C for 5 s, 40 cycles at 60 °C for 20 s, and one melting curve stage at 95 °C for 0 s, followed by 65 °C for 15 s and 95 °C for 0 s. The levels of expression of *wbbM*, *mrkA*, and *AcrA* were calculated using the $2^{-\Delta\Delta Ct}$ method [26].

## Statistical Analysis

Data were analyzed using GraphPad Prism v. 8.0 (GraphPad Software, La Jolla, CA, USA) and presented as the mean ± standard deviation. Multiple intergroup comparisons were performed using one-way analysis of variance (ANOVA). Differences between groups were evaluated by ANOVA followed by post-hoc test using the SPSS 22.0 software (IBM Corp., Armonk, NY, USA), A $P<0.05$ indicated statistically significant differences.

# Results

## hvKp Screening

Between October 2019 and October 2020, we collected a total of 289 clinical isolates of *K. pneumoniae* from the First Affiliated Hospital of Guangxi Medical University. Of the 289 K. *pneumoniae* strains, 80 were hvKp (27.68%), whereas 209 were cKp (72.32%).

## Source and Departmental Distribution of hvKp Specimens

Table 2 shows that the 80 hvKp strains originated mainly from the ICU (22.50%), respiratory medicine (22.50%), hepatobiliary surgery (10.00%), and neurosurgery (7.50%) departments. Table 3 shows that the 80 hvKp strains were

**Table 3** Source and distribution of hypervirulent *Klebsiella pneumoniae*

| Specimen | Value ($N=80$) |
|---|---|
| Sputum | 33 (41.25) |
| Alveolar lavage fluid | 16 (20.00) |
| Pharyngeal swab | 1 (1.25) |
| Pleural fluid | 2 (2.50) |
| Urine | 4 (5.00) |
| Drainage fluid | 2 (2.50) |
| Other secretions | 10 (12.5) |
| Bile | 4 (5.00) |
| Blood | 8 (10.00) |

Values are presented as No. (%) of isolates

primarily derived from sputum (41.25%), alveolar lavage fluid (20.00%), and other secretions (12.5%).

### Analysis of Biofilm Formation Ability

We identified that out of the 80 hvKp strains, 60 (75.00%) were biofilm-positive, whereas 20 (25.00%) were biofilm-negative. We also used crystal violet staining to analyze the biofilm formation ability of biofilm-positive strains. Figure 1b shows that based on ODc = 0.38, 18 (30.00%), 31 (51.67%), and 11 (18.33%) of the biofilm-positive hvKp strains were strong, moderate, and weak biofilm formers, respectively.

### Plotting of Biofilm Growth Curve

We determined that the carrier-attached biofilm mass was gradually increased from day 0, reaching its maximum on day 5 of incubation ($P < 0.05$) as indicated in Fig. 1c. On day 6 of incubation, we observed a slight decrease in the carrier-attached biofilm mass (P ˂ 0.05). On day 7, we did not detect any further decrease in the biofilm mass ($P > 0.05$). We further longitudinally analyzed the carrier-attached biofilm mass of the three clinical strains and *K. pneumoniae* ATCC43816. We found that hvKp1 generated the most biofilm mass on the carrier surface on days 3 and 5 ($P < 0.05$) as shown in Fig. 1d. Hence, we concluded that hvKp1 exhibited the highest biofilm formation capacity and used it in subsequent experiments.

### Biofilm Morphology Under Scanning Electron Microscopy

Biofilm morphologies of the three hvKp clinical strains and *K. pneumoniae* ATCC43816 are shown in Fig. 2. We specifically observed that after 1 d of in vitro culture, bacteria uniformly adhered to the carrier surface, exhibiting faintly visible hairs and bluntly rounded and rod-shaped morphology, with few of them being stacked. After 3 d of in vitro culture, we noticed that the bacteria were clustered into interconnected and stacked microcolonies, forming loose mesh-like 3D structures. In addition, we detected trace amounts of extracellular matrix and the emergence of an early biofilm pattern. After 5 d of in vitro culture, we found that the carrier surface was covered by a mature biofilm primarily consisting of rod-shaped bacteria arranged in a 3D-stacked layer and pore structure with abundant extracellular matrix. Finally, after 7 d of in vitro culture, we still observed the presence of a typical biofilm with mature morphology on the carrier surface.

### Determination of Minimum Inhibitory Concentration

The MICs of BA, EM, and LEV against the clinical isolate strain hvKp1 and standard strain *K. pneumoniae* ATCC43816 are shown in Table 4. We determined that both MICs of BA against the clinical isolate strain hvKp1 and standard strain *K. pneumoniae* ATCC43816 were > 2048 μg/ml. Likewise, we found that both MICs of EM against the either strains were > 32 μg/ml. In addition, we detected that the MICs of LEV against hvKp1 and *K. pneumoniae* ATCC43816 were > 0.25 and > 0.125 μg/ml, respectively.

### In Vitro Antibiofilm Effect

We treated our biofilm models on days 3 (d3) and 5 (d5) with BA alone or in combination with LEV for 24 h, using EM as a positive control. We evaluated the biofilm-forming inhibitory activity (antibiofilm effect) of these drugs using the plate count method and crystal violet staining (Fig. 3A). We detected that neither the biofilm mass on the carrier nor the bacterial counts inside the biofilm had significantly decreased in either biofilm models treated with BA, EM, LEV, and 2LEV ($P > 0.05$). Whereas, compared with the MH, BA, LEV, and 2LEV treatments, we found that BA + LEV and EM + LEV treatments significantly reduced the biofilm mass and bacterial counts inside the biofilm in the d3 biofilm model ($P < 0.05$). However, in the d5 biofilm model, neither the BA + LEV nor EM + LEV treatment had any significant effect on the biofilm mass or bacterial counts ($P > 0.05$). We also did not detect any significant differences between the BA + LEV and EM + LEV treatments in terms of biofilm mass or bacterial count ($P > 0.05$) in either of the biofilm models.

### Effects of Drug Treatment on hvKp Biofilm Morphology

We determined that early biofilm formation occurred after 3 d of in vitro culture, as shown in Fig. 4. We observed the morphologies of the generated biofilms under SEM after 24 h of drug treatment. In the MH and DMSO groups, we observed stereological structures typical of an early biofilm form, with small amounts of extracellular matrices being formed between the bacterial cells. Hence, we assumed that DMSO had no effect on biofilm formation. Interestingly, we found that after BA or EM treatment, hvKp bacterial titers were decreased, bacterial gaps were widened, and the amount of extracellular bacterial matrices was decreased. Whereas, we noticed that after the LEV and 2LEV treatments, the shape of bacteria was elongated, but the stereological structures of early biofilms were still visible. Finally, we found that in both the BA + LEV and EM + LEV

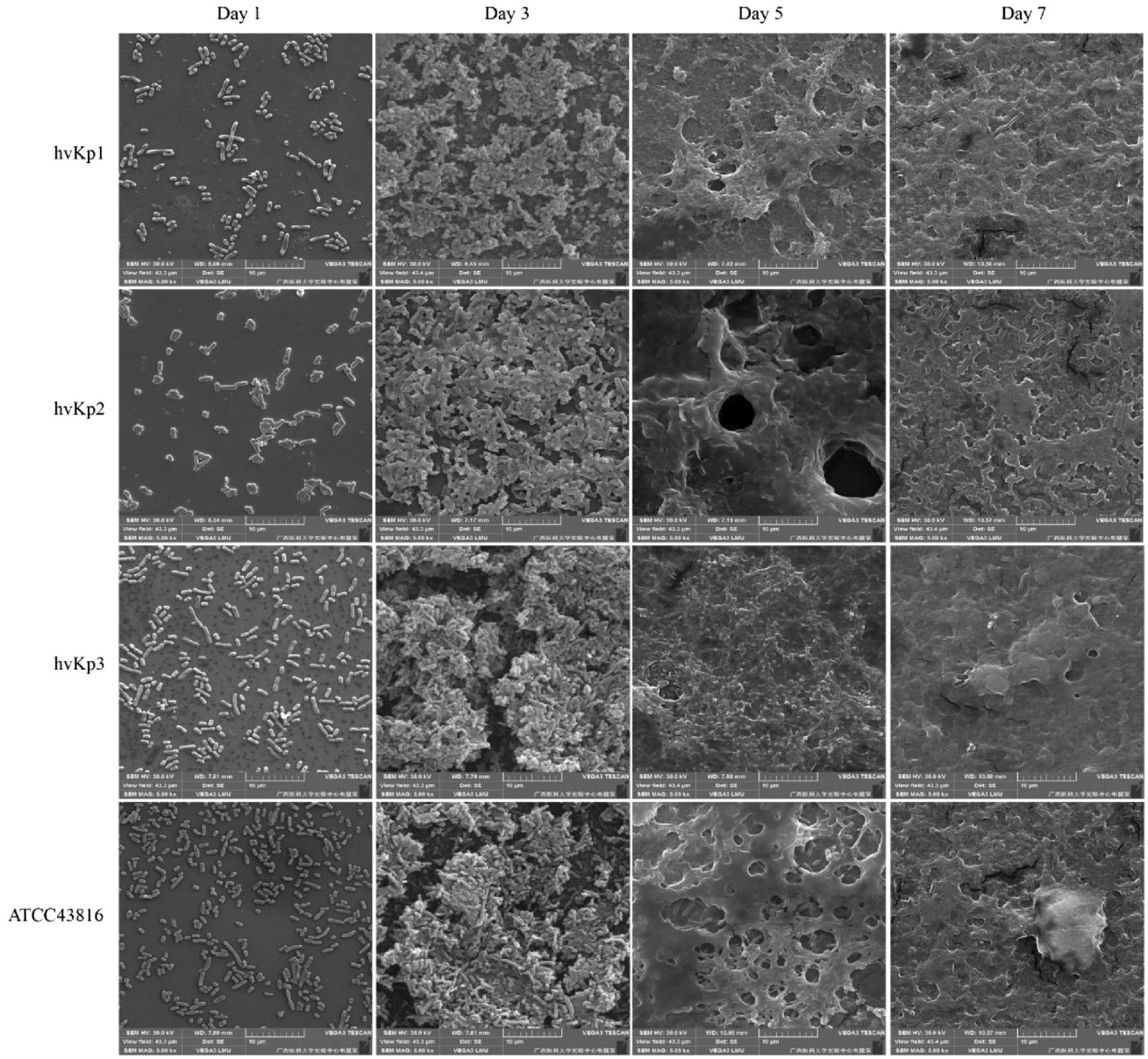


**Fig. 2** Dynamic observation of hypervirulent Klebsiella pneumoniae (hvKp) biofilm morphology under scanning electron microscope at × 5000

**Table 4** Baicalin, erythromycin, and levofloxacin minimum inhibitory concentrations (MICs) vs. hypervirulent *Klebsiella pneumoniae* (hvKp) 1 and ATCC43816

| Antimicrobial | MIC (μg/ml) | |
|---|---|---|
| | hvKp1 | ATCC43816 |
| Baicalin | 2048 | 2048 |
| Levofloxacin | 0.25 | 0.125 |
| Erythromycin | 32 | 32 |

treatments, the number of hvKp bacteria was significantly reduced, and the stereological structures had collapsed.

As mentioned, we observed the formation of a mature biofilm after 5 d of in vitro culture. We observed the morphologies of generated biofilms under SEM after 24 h drug treatment (Fig. 4). In cultures treated with MH, BA, EM, LEV, or 2LEV, we observed the typical morphology of mature biofilm, which was characterized by dense and viscous extracellular matrix and cellulosic material surrounding the bacteria. However, we noticed that the amount of extracellular matrices was slightly reduced, but the biofilm structures remained intact and three-dimensional in cultures treated with BA, EM, EM + LEV,

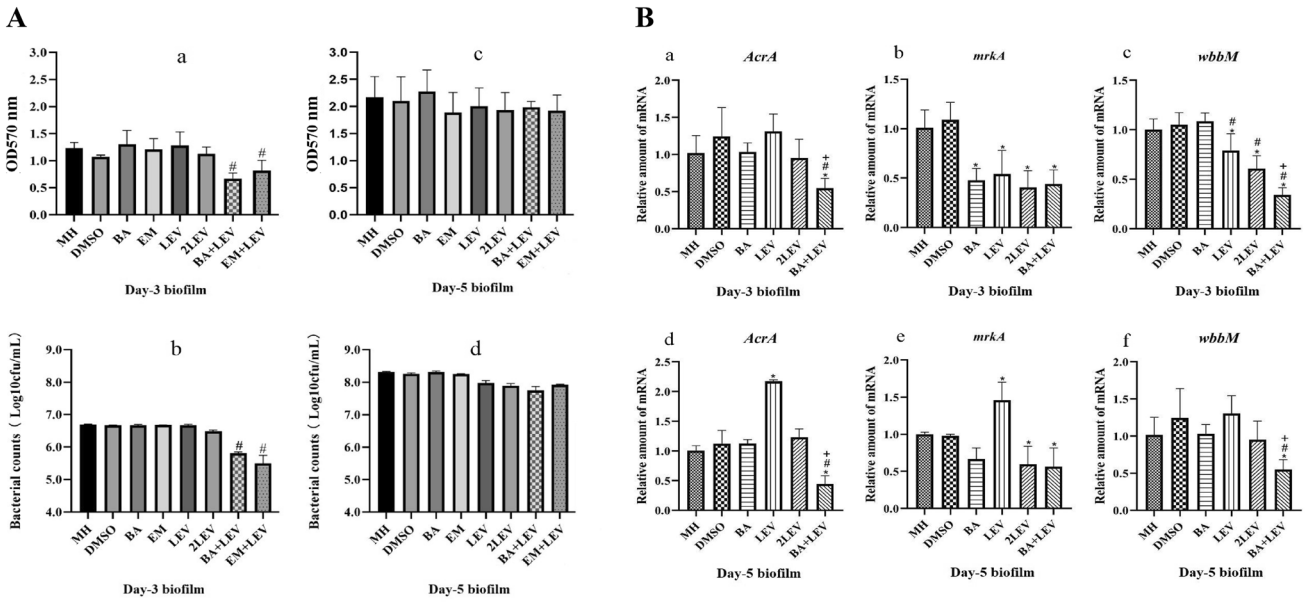


**Fig. 3** **A** Effect of baicalin (BA) plus levofloxacin (LEV) on biofilm mass and bacterial load of hypervirulent Klebsiella pneumoniae. # indicates $P<0.05$ compared with MH, BA, EM, LEV, or 2LEV treatment. **B** Effect of Baicalin combined Levofloxacin on the expression levels of hypervirulent Klebsiella pneumoniae biofilm-related regulatory genes. Note: *indicates $P<0.05$ compared to MH group; #indicates $P<0.05$ compared to BA group; + indicates $P<0.05$ compared to LEV group and 2LEV group

or BA + LEV. These findings were consistent with the results of the semiquantitative biofilm experiments based on crystal violet staining and enumeration of live serially diluted bacteria.

### Effects of Drug Treatments on Biofilm-Associated Gene Expression

We performed RT-qPCR to detect the relative levels of expression of the biofilm-associated genes *AcrA*, *mrkA*, and *wbbM* in hvKp treated with BA and LEV alone and in combination. We found that the combination of BA and LEV significantly inhibited the expression of these genes to a greater extent than either drug alone ($P>0.05$) as shown in Fig. 3B. Interestingly, we detected that at the early biofilm stage, treatment with BA, LEV, or 2LEV did not affect the expression of *AcrA* ($P>0.05$). Whereas, its expression was significantly downregulated in the BA + LEV group ($P>0.05$). We also determined that the expression of *wbbM* was inhibited in the LEV and 2LEV groups (P ˂ 0.05), Although BA alone did not affect the expression of *wbbM* ($P>0.05$), the combination of BA with LEV led to a significantly stronger inhibition in the expression of *wbbM* than that observed in the MH, BA, LEV, and 2LEV groups (P ˂ 0.05).

Notably, we observed that at the mature biofilm stage, treatment with BA and 2LEV groups did not affect the expression of *AcrA* ($P>0.05$). However, we detected that the expression of *AcrA* was upregulated after treatment with LEV ($P>0.05$), whereas significantly downregulated after combined treatment with BA and LEV ($P>0.05$). We found that, compared with MH, BA, LEV, and 2LEV had no effect on the expression of *wbbM* ($P>0.05$). Whereas, combined treatment with BA and LEV significantly downregulated the expression of *wbbM* ($P>0.05$) (Fig. 5).

## Discussion

The incidence of hvKp infections has steadily increased worldwide, widely varying in the Asia–Pacific region. In recent years, hvKp has emerged as a clinical variant of *K. pneumoniae* [8]. Although it is relatively more sensitive to antibiotics than cKp, hvKp is highly virulent, exhibiting a high capacity for biofilm formation [8]. To date, the identification of hvKp strains has been mainly based on the use of the "string test". Although hvKp exhibit a highly mucous phenotype strongly associated with high virulence and invasive infection, not all strains display the hypermucoviscous phenotype. Hence, proper definition of hvKp strains requires the use of the "string test" in conjunction with evaluation of clinical manifestations and detection of certain virulence genes. As no international standards for defining hvKp currently exist, most studies continue to use the "string test" to screen for hvKp strains [27]. In this study, we also used the "string test" to screen for hvKp among clinical strains of *K. pneumoniae*. Accordingly, the isolation rate of clinical hvKp at the

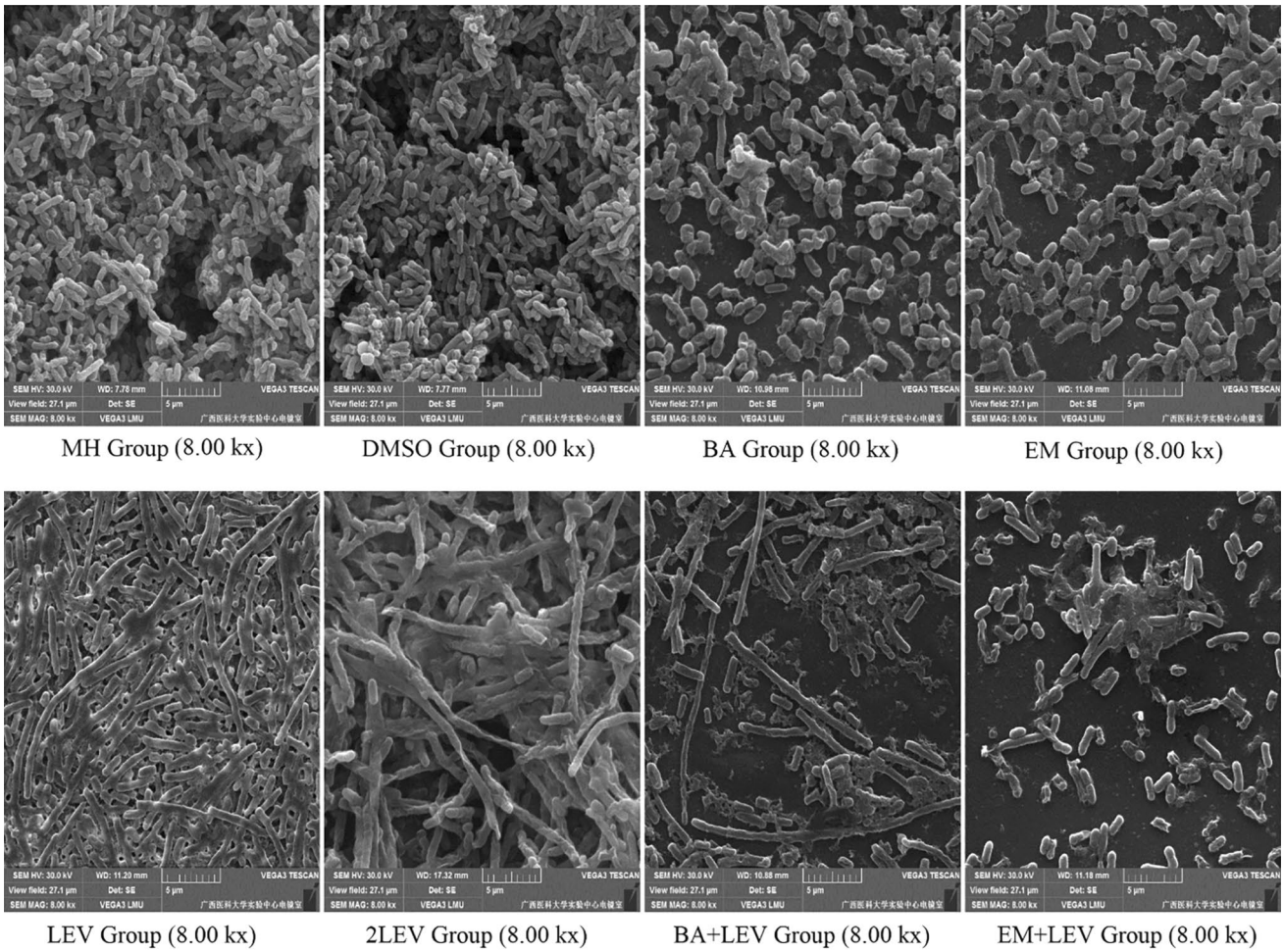


**Fig. 4** Effects of baicalin (BA) plus levofloxacin (LEV) on biofilm morphology. MH: Mueller–Hinton; DMSO: dimethyl sulfoxide; EM: erythromycin

First Affiliated Hospital of Guangxi Medical University between October 2019 and October 2020 was 27.68%. This incidence was slightly lower than those previously reported in the literature, possibly because our sources were more homogeneous, and our sample size was relatively smaller than those of earlier studies [28]. As such, the prevalence of hvKp might be underestimated due to the lack of objective diagnostic methods [29]. Moreover, hvKp was isolated mainly from the alveolar lavage fluid and sputum of patients in the respiratory medicine department and ICU, probably because these individuals might be immunocompromised and undergo frequent antibiotic administration and invasive surgery. Furthermore, hvKp appears to primarily cause respiratory infections. Sputum is prone to contamination from colonizing bacteria. Hence, health care professionals should improve the collection and management of sputum specimens by handling sample preparation, preservation, and delivery aseptically.

There have been relatively more studies on biofilm formation by *Staphylococcus aureus*, *Pseudomonas aeruginosa*, and *Candida albicans* than on biofilm formation by hvKp. Here, we assessed the biofilm formation ability of 80 hvKp strains and found that among 60 biofilm-positive strains, 18 (30.00%), 31 (51.67%), and 11 (18.33%) were strong, moderate, and weak biofilm formers, respectively. Thus, hvKp has a strong overall ability for biofilm formation. Bacteria can attach to biological materials, latex, stainless steel, silicon, glass, polycarbonate, PVC, and other nonbiological materials and form biofilm on them [30]. The generation of artificial biofilm helps clarify the mechanisms of its formation and biological activity and can be used for the establishment of later-stage in vivo infection [31]. We found that hvKp strains underwent attachment, aggregation, maturation, and dispersal until the next round of attachment. Notably, hvKp formed early and mature biofilms in vitro after 3 and 5 days of continuous culture, respectively. The modelling method used herein was characterized by simple

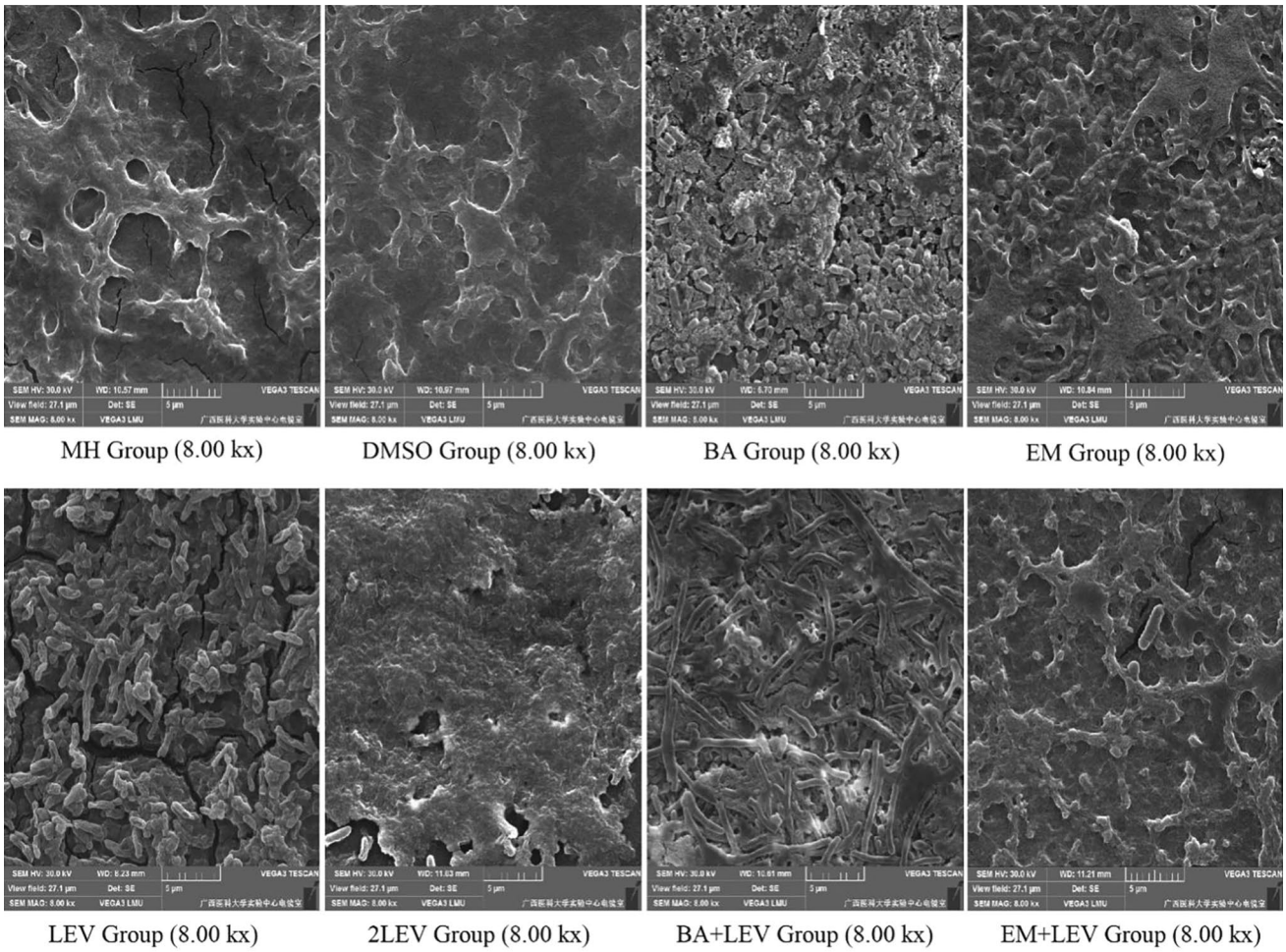


**Fig. 5** Effects of baicalin (BA) plus levofloxacin (LEV) on mature biofilm morphology. MH: Mueller–Hinton; DMSO: dimethyl sulfoxide; EM: erythromycin

operation, ready availability of materials, short culture period, and high stability. Therefore, we successfully established an in vitro quiescent model for hvKp and provided a theoretical basis for investigating hvKp biofilm-associated infections.

Bacterial biofilms contribute to virulence and chronic infection. A biofilm provides a favorable inert environment that confers antibiotic resistance to the planktonic bacteria that are embedded deeper in the structure [30]. In recent years, combinations of multiple antibiotics have been administered to treat biofilm-associated bacterial infections. However, these drug combinations are not viable long-term treatment options, and new therapeutic strategies are urgently needed.

Erythromycin inhibits biofilm formation and the production of virulence factors, such as protein hydrolase, elastase, and rhamnolipids in *Pseudomonas aeruginosa*. Combined with ceftazidime, imipenem, or LEV, EM has been reported to exert coordinated antibacterial efficacy against *P. aeruginosa* biofilms [32, 33]. We thus established in vitro models of early and mature hvKp biofilms based on this foregoing approach. We used EM as a positive control to investigate the toxic effects of BA alone or in combination with LEV on hvKp biofilms. The mass of early and mature biofilm on the carrier surface and number of bacteria within the biofilm did not decrease after LEV or 2LEV treatment. In contrast, the combination of LEV plus BA or EM effectively cleared the early biofilm, killed the resident bacteria, and loosened the biofilm structure. However, the same drug combinations had comparatively lower efficacy against the mature biofilm. Moreover, treatment with either BA + LEV or EM + LEV did not significantly differ in their efficacy against early or mature biofilm. Therefore, we assumed that BA and EM might have comparable antibiofilm efficacy.

Importantly, hvKp has various virulence factors, including bacterial hairs, lipopolysaccharides (LPS), efflux pumps, and iron carriers, which protect the pathogen against host immune responses and antibiotics and strengthen its

adhesion to epithelial tissues and medical device surfaces [8]. Several virulence genes implicated in biofilm formation, such as *AcrA*, *mrkA*, and *wbbM*, were detected in *K. pneumoniae* [22]. The multidrug efflux pump of gram-negative bacilli is a bacterial defense mechanism. Thus, efflux pump upregulation often causes multidrug resistance in bacteria and is a key factor in emerging global antibiotic resistance [34]. The efflux pump system has been associated with both antibiotic resistance and biofilm formation [35]. The AcrAB-TolC system and its homologs are the main multidrug efflux transporters in gram-negative bacilli [36]. Type I and III hairs on *K. pneumoniae* have been associated with biofilm formation and chronic urinary tract infections. *mrkA* and *mrkD* are adhesion genes encoding type III hairs [37, 38]. In addition, the MrkA protein in the type III hair complex has been associated with biofilm formation [39]. Thus, hvKp strains expressing *mrkA*, *mrkD*, and *rmpA* might have moderate to strong biofilm formation capabilities [40].

Lipopolysaccharides, which consist of polysaccharides and lipids, are the main components of the outer cell wall in gram-negative bacilli, and act as endotoxins, causing fever in humans [41]. Of note, LPS have been closely associated with biofilm formation [42]. The D-galactose I biosynthetic gene cluster in *K. pneumoniae* encodes the predicted galactosyltransferases WbbM, WbbN, and WbbO [43]. However, there is only conclusive empirical evidence for WbbO and WbbM. The latter is a newly identified O2a antigen polymerase closely associated with LPS biosynthesis [44]. We used RT-PCR to investigate the effects of BA plus LEV on the expression of hvKp biofilm-associated genes. The combination of BA and LEV significantly downregulated the expression of *AcrA* and *wbbM* in both early and mature biofilms. When LEV alone was applied to the mature biofilm at MIC concentrations, the expression of *AcrA* was significantly upregulated compared with that in the MH group. In contrast, when LEV was applied in combination with BA to the mature biofilm at MIC concentrations, the expression of *AcrA* was significantly downregulated compared with that in the MH group. These observations were consistent with those of previous studies [45]. Low antibiotic doses have been shown to not be able to downregulate the expression of genes encoding the efflux pump system; however, they do upregulate the expression of its regulatory genes. Previous studies proposed that BA inhibits the efflux pump system and, by extension, biofilm formation [46, 47]. Similar results in the present study indicated that BA might, therefore, inhibit the efflux pump system in hvKp biofilms. Therefore, the employment of such drug combination treatments might be an effective therapeutic strategy for improving the management of hvKp biofilm-associated infections.

## Conclusions

The present study showed that the isolation rate of clinical hvKp strains at the First Affiliated Hospital of Guangxi Medical University was 27.86%. Most hvKp strains were isolated from the sputum and alveolar lavage fluid of patients in the respiratory medicine department and ICU. We successfully established a static hvKp biofilm model in vitro and detected the formation of early and mature biofilms after only 3 and 5 d of continuous culture, respectively. Importantly, hvKp strains exhibited a strong biofilm formation ability. However, administration of BA significantly disrupted the formed hvKp biofilm and cooperated with LEV to enter the biofilm structure and exert its bactericidal function. Moreover, the combination of BA with LEV had higher efficacy against early than mature biofilm, which was comparable to that of EM. Thus, BA plus LEV might be effective against the formation of hvKp biofilms by affecting the transcription of genes regulating the efflux pump system. This drug combination treatment might represent a novel strategy for enhancing the efficacy of treatments by reducing biofilm-associated drug resistance. As a new drug against bacterial diseases, which has been shown to reduce the virulence of bacterial strains, BA and its mechanisms of action require further investigation in future research.

**Supplementary Information** The online version contains supplementary material available at https://doi.org/10.1007/s00284-023-03226-y.

**Acknowledgements** We are thankful to the Centre for Environmental Life Sciences Engineering Laboratory, Nanyang Technological University, Singapore for gifting us the *K. pneumoniae* ATCC43816 strain.

**Author Contributions** All operations performed by JH were done under the guidance of YC. YY was responsible for collecting samples and testing. With the assistance of TL, JH compiled all the data and wrote this manuscript. All authors read and approved the final manuscript.

**Funding** This work was supported by the National Natural Science Foundation of China [Grant Number 82104499]; Guangxi Health Commission Key Lab of Fungi and Mycosis Research and Prevention [Grant Number ZZH2020004]; The First Affiliated Hospital of Guangxi Medical University Provincial and Ministerial Key Laboratory Cultivation Project: Guangxi Key Laboratory of Tropical Fungi and Mycosis Research [Grant Number YYZS2020006]; and Guangxi Health Commission Self-financing Project [Grant Number Z20210909].

**Data Availability** Not applicable.

## Declarations

**Competing interest** The authors declare that they have no competing interests.

**Ethical Approval** The study was approved by the Ethics Committee of the First Affiliated Hospital of Guangxi Medical University (Approval Number: 2022-E404-05).

**Consent to Participate** Written informed consent for the provision and release of all clinical samples used in the study was obtained from all participants.

## References


1. Wong Fok Lung T, Charytonowicz D, Beaumont KG et al (2022) Klebsiella pneumoniae induces host metabolic stress that promotes tolerance to pulmonary infection. Cell Metab 34:761-774.e9. https://doi.org/10.1016/j.cmet.2022.03.009
2. Wang G, Zhao G, Chao X, Xie L, Wang H (2020) The Characteristic of virulence, biofilm and antibiotic resistance of *Klebsiella pneumoniae*. Int J Environ Res Public Health 17:6278. https://doi.org/10.3390/ijerph17176278
3. Zhang Y, Yao Z, Zhan S, Yang Z, Wei D, Zhang J, Li J, Kyaw MH (2014) Disease burden of intensive care unit-acquired pneumonia in China: a systematic review and meta-analysis. Int J Infect Dis 29:84–90. https://doi.org/10.1016/j.ijid.2014.05.030
4. Chew KL, Lin RTP, Teo JWP (2017) *Klebsiella pneumoniae* in Singapore: Hypervirulent Infections and the Carbapenemase Threat. Front Cell Infect Microbiol 7:515. https://doi.org/10.3389/fcimb.2017.00515
5. Russo TA, Olson R, Fang CT, Stoesser N, Miller M, MacDonald U, Hutson A, Barker JH, La Hoz RM, Johnson JR (2018) Identification of biomarkers for differentiation of hypervirulent Klebsiella pneumoniae from classical K. pneumoniae. J Clin Microbiol 56:e00776-e818. https://doi.org/10.1128/JCM.00776-18
6. Nassif X, Fournier JM, Arondel J, Sansonetti PJ (1989) Mucoid phenotype of Klebsiella pneumoniae is a plasmid-encoded virulence factor. Infect Immun 57:546–552. https://doi.org/10.1128/iai.57.2.546-552.1989
7. Liu Y, Cheng DL, Lin CL (1986) Klebsiella pneumoniae liver abscess associated with septic endophthalmitis. Arch Intern Med 146:1913–1916. https://doi.org/10.1001/archinte.1986.00360220057011
8. Russo TA, Marr CM (2019) Hypervirulent Klebsiella pneumoniae. Clin Microbiol Rev 32:e00001-19. https://doi.org/10.1128/CMR.00001-19
9. Edgar L, Pu T, Porter B, Aziz JM, La Pointe C, Asthana A, Orlando G (2020) Regenerative medicine, organ bioengineering and transplantation. Br J Surg 107:793–800. https://doi.org/10.1002/bjs.11686
10. Cometta S, Jones RT, Juárez-Saldivar A et al (2022) Melimine-modified 3D-printed polycaprolactone scaffolds for the prevention of biofilm-related biomaterial infections. ACS Nano 16:16497–16512. https://doi.org/10.1021/acsnano.2c05812
11. Arciola CR, Campoccia D, Montanaro L (2018) Implant infections: adhesion, biofilm formation and immune evasion. Nat Rev Microbiol 16:397–409. https://doi.org/10.1038/s41579-018-0019-y
12. Hall CW, Mah TF (2017) Molecular mechanisms of biofilm-based antibiotic resistance and tolerance in pathogenic bacteria. FEMS Microbiol Rev 41:276–301. https://doi.org/10.1093/femsre/fux010
13. Jukič M, Bren U (2022) Machine learning in antibacterial drug design. Front Pharmacol 13:864412. https://doi.org/10.3389/fphar.2022.864412
14. Arya SS, Sharma MM, Das RK, Rookes J, Cahill D, Lenka SK (2019) Heliyon 5:e02021. https://doi.org/10.1016/j.heliyon.2019.e02021
15. Leung KC, Seneviratne CJ, Li X, Leung PC, Lau CB, Wong CH, Pang KY, Wong CW, Wat E, Jin L (2016) Synergistic antibacterial effects of nanoparticles encapsulated with Scutellaria baicalensis and pure chlorhexidine on oral bacterial biofilms. Nanomaterials 6:61. https://doi.org/10.3390/nano6040061
16. Huang T, Liu Y, Zhang C (2019) Pharmacokinetics and bioavailability enhancement of baicalin: a review. Eur J Drug Metab Pharmacokinet 44:159–168. https://doi.org/10.1007/s13318-018-0509-3
17. Du Z, Huang Y, Chen Y, Chen Y (2019) Combination effects of baicalin with levofloxacin against biofilm-related infections. Am J Transl Res 11:1270–1281
18. Bush NG, Diez-Santos I, Abbott LR, Maxwell A (2020) Quinolones: mechanism, lethality and their contributions to antibiotic resistance. Molecules 25:5662. https://doi.org/10.3390/molecules25235662
19. Pu Y, Pan J, Yao Y, Ngan WY, Yang Y, Li M, Habimana O (2021) Ecotoxicological effects of erythromycin on a multispecies biofilm model, revealed by metagenomic and metabolomic approaches. Environ Pollut 276:116737. https://doi.org/10.1016/j.envpol.2021.116737
20. Shendurnikar N (1988) Erythromycin. Indian Pediatr 25:780–783
21. Sayeed MA, Latif N, Mahmood SF (2017) Hypermucoviscous Klebsiella syndrome it's in the community! J Pak Med Assoc 67:1930–1932
22. Vuotto C, Longo F, Pascolini C, Donelli G, Balice MP, Libori MF, Tiracchia V, Salvia A, Varaldo PE (2017) Biofilm formation and antibiotic resistance in Klebsiella pneumoniae urinary strains. J Appl Microbiol 123:1003–1018. https://doi.org/10.1111/jam.13533
23. Chantell C, Humphries RM, Lewis II JS (2019) Clinical and laboratory standards institute**,** fluoroquinolone breakpoints for enterobacteriaceae and pseudomonas aeruginosa**.** CLSI Rationale: document MR02. CLSI, Wayne
24. Herigstad B, Hamilton M, Heersink J (2001) How to optimize the drop plate method for enumerating bacteria. J Microbiol Methods 44:121–129. https://doi.org/10.1016/s0167-7012(00)00241-4
25. Coffey BM, Anderson GG (2014) Biofilm formation in the 96-well microtiter plate. Methods Mol Biol 1149:631–641. https://doi.org/10.1007/978-1-4939-0473-0_48
26. Schmittgen TD, Livak KJ (2008) Analyzing real-time PCR data by the comparative C(T) method. Nat Protoc 3:1101–1108. https://doi.org/10.1038/nprot.2008.73
27. Catalán-Nájera JC, Garza-Ramos U, Barrios-Camacho H (2017) Hypervirulence and hypermucoviscosity: Two different but complementary Klebsiella spp. phenotypes? Virulence 8:1111–1123. https://doi.org/10.1080/21505594.2017.1317412
28. Zhang Y, Zhao C, Wang Q, Wang X, Chen H, Li H, Zhang F, Li S, Wang R, Wang H (2016) High prevalence of hypervirulent Klebsiella pneumoniae infection in China: geographic distribution, clinical characteristics, and antimicrobial resistance. Antimicrob Agents Chemother 60:6115–6120. https://doi.org/10.1128/AAC.01127-16
29. Yang Y, Liu JH, Hu XX, Zhang W, Nie TY, Yang XY, Wang XK, Li CR, You XF (2020) Clinical and microbiological characteristics of hypervirulent Klebsiella pneumoniae (hvKp) in a hospital from North China. J Infect Dev Ctries 14:606–613. https://doi.org/10.3855/jidc.12288
30. Ling N, Forsythe S, Wu Q, Ding Y, Zhang J, Zeng H (2020) Insights into Cronobacter sakazakii biofilm formation and control strategies in the food industry. Engineering 6:393–405. https://doi.org/10.1016/j.eng.2020.02.007

31. Singla S, Harjai K, Chhibber S (2014) Artificial Klebsiella pneumoniae biofilm model mimicking in vivo system: altered morphological characteristics and antibiotic resistance. J Antibiot 67:305–309. https://doi.org/10.1038/ja.2013.139
32. Xu Z, Liu F, Wang X (2001) Effects of erythromycin and fosfomycin on pseudomonas aeruginosa biofilm in vitro. Zhonghua Jie He Hu Xi Za Zhi 24:342–344
33. Guan Y, Li C, Shi JJ, Zhou HN, Liu L, Wang Y, Pu YP (2013) Effect of combination of sub-MIC sodium houttuyfonate and erythromycin on biofilm of staphylococcus epidermidis. Zhongguo Zhong Yao Za Zhi 38:731–735
34. Müller RT, Pos KM (2015) The assembly and disassembly of the AcrAB-TolC three-component multidrug efflux pump. Biol Chem 396:1083–1089. https://doi.org/10.1515/hsz-2015-0150
35. Heacock-Kang Y, Sun Z, Zarzycki-Siek J, Poonsuk K, McMillan IA, Chuanchuen R, Hoang TT (2018) Two regulators, PA3898 and PA2100, modulate the pseudomonas aeruginosa multidrug resistance MexAB-OprM and EmrAB efflux pumps and biofilm formation. Antimicrob Agents Chemother 62:e01459-e1518. https://doi.org/10.1128/AAC.01459-18
36. Ugwuanyi FC, Ajayi A, Ojo DA, Adeleye AI, Smith SI (2021) Evaluation of efflux pump activity and biofilm formation in multidrug resistant clinical isolates of Pseudomonas aeruginosa isolated from a Federal Medical Center in Nigeria. Ann Clin Microbiol Antimicrob 20:11. https://doi.org/10.1186/s12941-021-00417-y
37. Tang M, Wei X, Wan X, Ding Z, Ding Y, Liu J (2020) The role and relationship with efflux pump of biofilm formation in Klebsiella pneumoniae. Microb Pathog 147:104244. https://doi.org/10.1016/j.micpath.2020.104244
38. Langstraat J, Bohse M, Clegg S (2001) Type 3 fimbrial shaft (MrkA) of Klebsiella pneumoniae, but not the fimbrial adhesin (MrkD), facilitates biofilm formation. Infect Immun 69:5805–5812. https://doi.org/10.1128/IAI.69.9.5805-5812.2001
39. Alkhudhairy MK, Alshadeedi SMJ, Mahmood SS, Al-Bustan SA, Ghasemian A (2019) Comparison of adhesin genes expression among Klebsiella oxytoca ESBL-non-producers in planktonic and biofilm mode of growth, and imipenem sublethal exposure. Microb Pathog 134:103558. https://doi.org/10.1016/j.micpath.2019.103558
40. Bakhtiari R, Javadi A, Aminzadeh M, Molaee-Aghaee E, Shaffaghat Z (2021) Association between presence of RmpA, MrkA and MrkD genes and antibiotic resistance in clinical Klebsiella pneumoniae isolates from hospitals in Tehran. Iran. Iran J Public Health 50:1009–1016. https://doi.org/10.18502/ijph.v50i5.6118
41. Maldonado RF, Sá-Correia I, Valvano MA (2016) Lipopolysaccharide modification in Gram-negative bacteria during chronic infection. FEMS Microbiol Rev 40:480–493. https://doi.org/10.1093/femsre/fuw007
42. Wasfi R, Hamed SM, Amer MA, Fahmy LI (2020) Proteus mirabilis biofilm: development and therapeutic strategies. Front Cell Infect Microbiol 10:414. https://doi.org/10.3389/fcimb.2020.00414
43. Kos V, Whitfield C (2010) A membrane-located glycosyltransferase complex required for biosynthesis of the D-galactan I lipopolysaccharide O antigen in Klebsiella pneumoniae. J Biol Chem 285:19668–19687. https://doi.org/10.1074/jbc.M110.122598
44. Clarke BR, Ovchinnikova OG, Sweeney RP, Kamski-Hennekam ER, Gitalis R, Mallette E, Kelly SD, Lowary TL, Kimber MS, Whitfield C (2020) A bifunctional O-antigen polymerase structure reveals a new glycosyltransferase family. Nat Chem Biol 16:450–457. https://doi.org/10.1038/s41589-020-0494-0
45. Chetri S, Bhowmik D, Dhar D, Chakravarty A, Bhattacharjee A (2019) Effect of concentration gradient carbapenem exposure on expression of blaNDM-1 and acrA in carbapenem resistant *Escherichia coli*. Infect Genet Evol 73:332–336. https://doi.org/10.1016/j.meegid.2019.05.024
46. Huang YQ, Huang GR, Wu MH et al (2015) Inhibitory effects of emodin, baicalin, schizandrin and berberine on hefA gene: treatment of Helicobacter pylori-induced multidrug resistance. World J Gastroenterol 21:4225–4231. https://doi.org/10.3748/wjg.v21.i14.4225
47. Wang J, Jiao H, Meng J, Qiao M, Du H, He M, Ming K, Liu J, Wang D, Wu Y (2019) Baicalin inhibits biofilm formation and the quorum-sensing system by regulating the MsrA drug efflux pump in Staphylococcus saprophyticus. Front Microbiol 10:2800. https://doi.org/10.3389/fmicb.2019.02800